

Effect of Ball Milling on the Electrochemical Performance of $\text{Li}_{1.02}\text{Ni}_{0.4}\text{Co}_{0.2}\text{Mn}_{0.4}\text{O}_2$ Cathode Synthesized by Citric Acid-Assisted Sol-Gel Process

R. Santhanam, Sundara. L. Ghatty, B. Rambabu*

Solid State Ionics and Surface Sciences Lab, Department of Physics, Southern University, Baton Rouge, LA 70813, USA

*E-mail: rambabu@cox.net

Received: 30 December 2009 / Accepted: 25 February 2010 / Published: 28 February 2010

Layered-type $\text{Li}_{1.02}\text{Ni}_{0.4}\text{Co}_{0.2}\text{Mn}_{0.4}\text{O}_2$ material has been synthesized by citric acid -assisted sol gel process. The resulting material was characterized by X-ray diffraction, scanning electron microscopy, charge-discharge measurements and impedance spectroscopy. The cathodes were prepared with carbon by hand grinding and ball milling. At a 0.1 C- rate and between 2.5 and 4.3 V, the hand-ground and ball-milled $\text{Li}_{1.02}\text{Ni}_{0.4}\text{Co}_{0.2}\text{Mn}_{0.4}\text{O}_2$ samples delivered a first-cycle discharge capacity of 156 mAh/g and 167 mAh/g, respectively. At a high C-rate of 8C, the ball-milled sample gave a capacity of 133 mAh/g which was significantly higher than the capacity obtained from hand-ground sample (115 mAh/g). In a 50-cycle test at 8C, the capacity retention of hand-ground and ball-milled samples was calculated as 75% and 87%, respectively. Ball milling the active material with carbon resulted in enhanced capacity, rate capability and cycleability due to significant decrease in the contact resistance between $\text{Li}_{1.02}\text{Ni}_{0.4}\text{Co}_{0.2}\text{Mn}_{0.4}\text{O}_2$ and carbon particles.

Keywords: lithium metal oxide, sol-gel method, ball milling, lithium batteries

1. INTRODUCTION

Since the commercial introduction of lithium ion batteries about 15 years ago by Sony, LiCoO_2 has been the dominating cathode material [1]. This material has several advantages such as ease of preparation, high capacity, good rate capability and high electronic conductivity [2, 3]. However, concerns over high cost of cobalt, toxicity, dissolution of Co, inherent safety problems, and buildup of impedance during cycling have led a prolonged effort to find alternative cathode materials for the advanced lithium-ion batteries [4-6]. Recently, transition metal layered oxides of composition $\text{LiNi}_{1-x-y}\text{Co}_x\text{Mn}_y\text{O}_2$ have been extensively studied for high capacity, rate capability, thermal stability and long

cycle life. Among them, $\text{LiNi}_{1/3}\text{Co}_{1/3}\text{Mn}_{1/3}\text{O}_2$, $\text{LiNi}_{0.5}\text{Mn}_{0.5}\text{O}_2$ and $\text{LiNi}_{0.4}\text{Co}_{0.2}\text{Mn}_{0.4}\text{O}_2$ cathode materials have been widely studied and are capable of delivering in excess of 155 mAh/g when cycled to 4.3V and over 200 mAh/g to potentials above 4.6V [7-14].

In order to improve the electrochemical performance of the layered type materials, extensive studies have been carried out to improve the performance of the cathode active materials by cationic substitution. Among them, electrochemically inert metals such as Al, Mg, Zn, Ti, Fe and Zr [15-21] have been used for partial substitution of Ni or Co to enhance the electrochemical performance of the cathode since they have shown beneficial effects for the suppression of phase transitions and lattice changes during charge–discharge cycling. An alternate approach to improve electrochemical performance is to change the surface properties of the cathode material by coating its particle with some metal oxides. The surface modifications of various layered oxides have been pursued extensively with various coating materials including Al_2O_3 , TiO_2 , ZrO_2 , and AlPO_4 [22-25]. This modification is believed to reduce reaction of electrodes with electrolyte at charged states since the inactive coating layer prevents the electrode from direct contact with electrolyte.

Since layered oxide materials have low electronic conductivity, it has to be mixed with a conducting additive such as carbon powder to increase the electronic conductivity of the working cathode. It has been reported that ball milling process improved the cycle life of the spinel LiMn_2O_4 cathode materials for rechargeable lithium ion batteries [26-28]. In this paper, we report the preparation and electrochemical behavior of layered $\text{Li}_{1.02}\text{Ni}_{0.4}\text{Co}_{0.2}\text{Mn}_{0.4}\text{O}_2$ cathode material ball milled with carbon. The results are compared with the cathode material hand ground with carbon. Our results here will show that a simple ball milling processing procedure can be advantageous to capacity, rate capability and cycleability of the layered $\text{Li}_{1.02}\text{Ni}_{0.4}\text{Co}_{0.2}\text{Mn}_{0.4}\text{O}_2$ cathode material.

2. EXPERIMENTAL PART

$\text{Li}_{1.02}\text{Ni}_{0.4}\text{Co}_{0.2}\text{Mn}_{0.4}\text{O}_2$ cathode material was synthesized by the citric acid sol-gel method [28, 29]. Stoichiometric amounts of $\text{Li}(\text{CH}_3\text{COO})\cdot 2\text{H}_2\text{O}$, $\text{Mn}(\text{CH}_3\text{COO})_2\cdot 4\text{H}_2\text{O}$, $\text{Ni}(\text{CH}_3\text{COO})_2\cdot 4\text{H}_2\text{O}$, and $\text{Co}(\text{CH}_3\text{COO})_2\cdot 4\text{H}_2\text{O}$ were dissolved in distilled water. Citric acid was used as a chelating agent. The solution pH was adjusted to 7.0 with ammonium hydroxide. The solution was heated at 70–80°C until a transparent sol was obtained. The resulting gel precursor was dried at 120°C for 4 h in air and followed with decomposition at 450°C for 8 h to remove the organic contents. The decomposed powders were ground, and sintered at 850°C in air for 12 h. The heating rate of the powder was 2°C/min. The as prepared $\text{Li}_{1.02}\text{Ni}_{0.4}\text{Co}_{0.2}\text{Mn}_{0.4}\text{O}_2$ powder was mixed with carbon in the weight ratio of 80: 10 by ball milling (Spex 8000 Mixer/Mill) with stainless steel balls for 2h. For comparison, $\text{Li}_{1.02}\text{Ni}_{0.4}\text{Co}_{0.2}\text{Mn}_{0.4}\text{O}_2$ powder was also prepared by the sol-gel process as described above and mixed with carbon by hand grinding. Hereafter, the ball milled and hand ground $\text{Li}_{1.02}\text{Ni}_{0.4}\text{Co}_{0.2}\text{Mn}_{0.4}\text{O}_2$ samples with carbon are designated as BM- $\text{Li}_{1.02}\text{Ni}_{0.4}\text{Co}_{0.2}\text{Mn}_{0.4}\text{O}_2$ and HG- $\text{Li}_{1.02}\text{Ni}_{0.4}\text{Co}_{0.2}\text{Mn}_{0.4}\text{O}_2$, respectively.

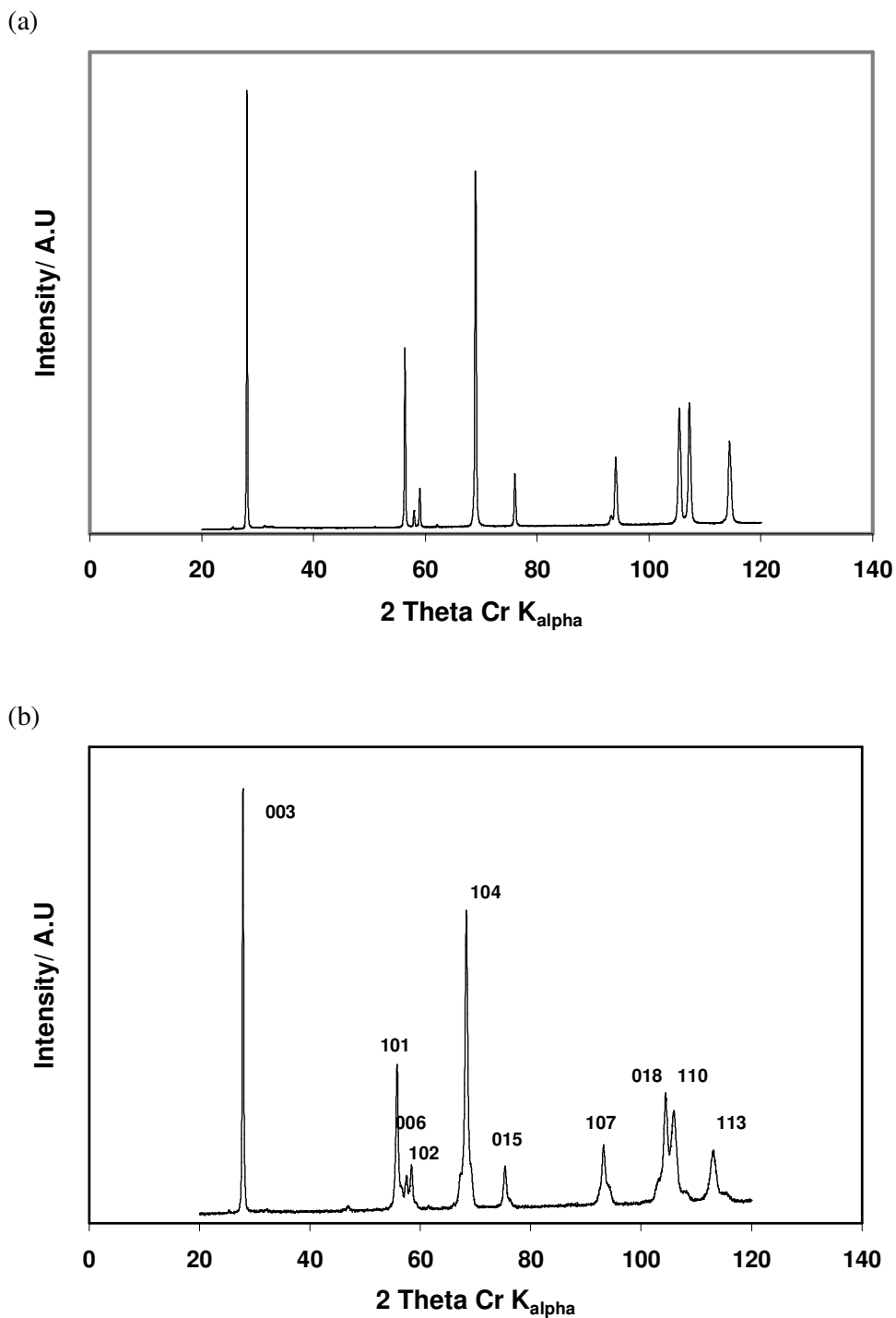
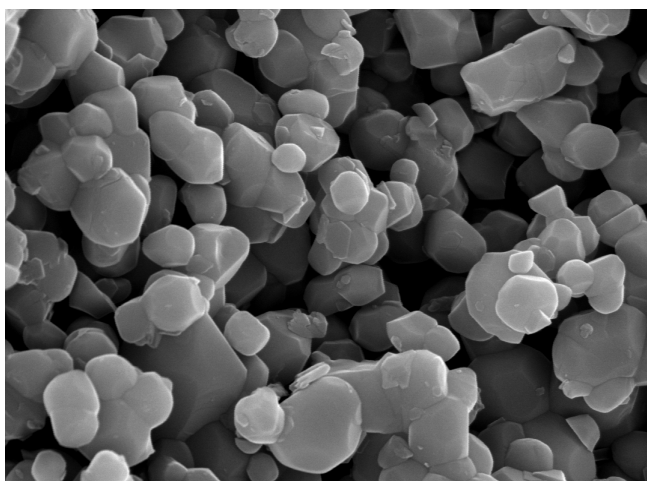


Figure 1. X-ray diffraction patterns of (a) HG- Li_{1.02}Ni_{0.4}Co_{0.2}Mn_{0.4}O₂, and (b) BM- Li_{1.02}Ni_{0.4}Co_{0.2}Mn_{0.4}O₂ cathodes.

The Li, Co, Ni and Mn contents in the resulting materials were analyzed using an inductively coupled plasma/atomic emission spectrometer (ICP/AES). The measured composition of the materials is close to the target composition so that the nominal compositions are used to describe the materials

throughout this paper for simplicity. The phase purity was verified from powder X-ray diffraction (XRD) measurements. It should be noted Cr K α X-ray source was used in this work. Therefore, the peak positions obtained from Cu K α X-ray source are different from the peaks positions obtained from this work. The particle morphology of the powders after sintering was obtained using a scanning electron microscopy (SEM).

(a)

X 30.0k $\overline{1\mu\text{m}}$

(b)

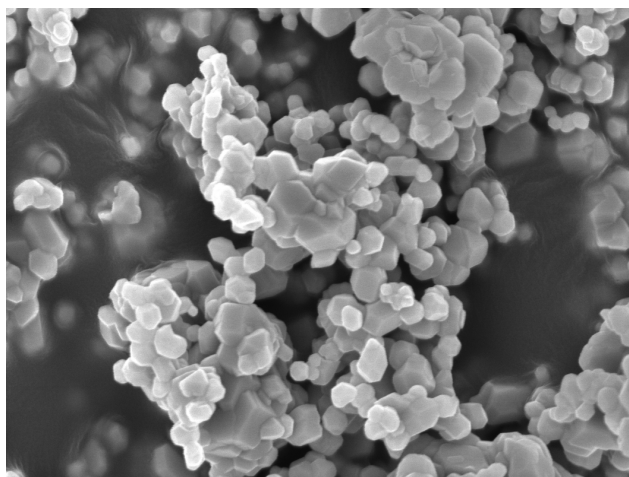
X 30.0k $\overline{1\mu\text{m}}$

Figure 2. SEM photograph of (a) HG-Li_{1.02}Ni_{0.4}Co_{0.2}Mn_{0.4}O₂, and (b) BM-Li_{1.02}Ni_{0.4}Co_{0.2}Mn_{0.4}O₂ cathodes.

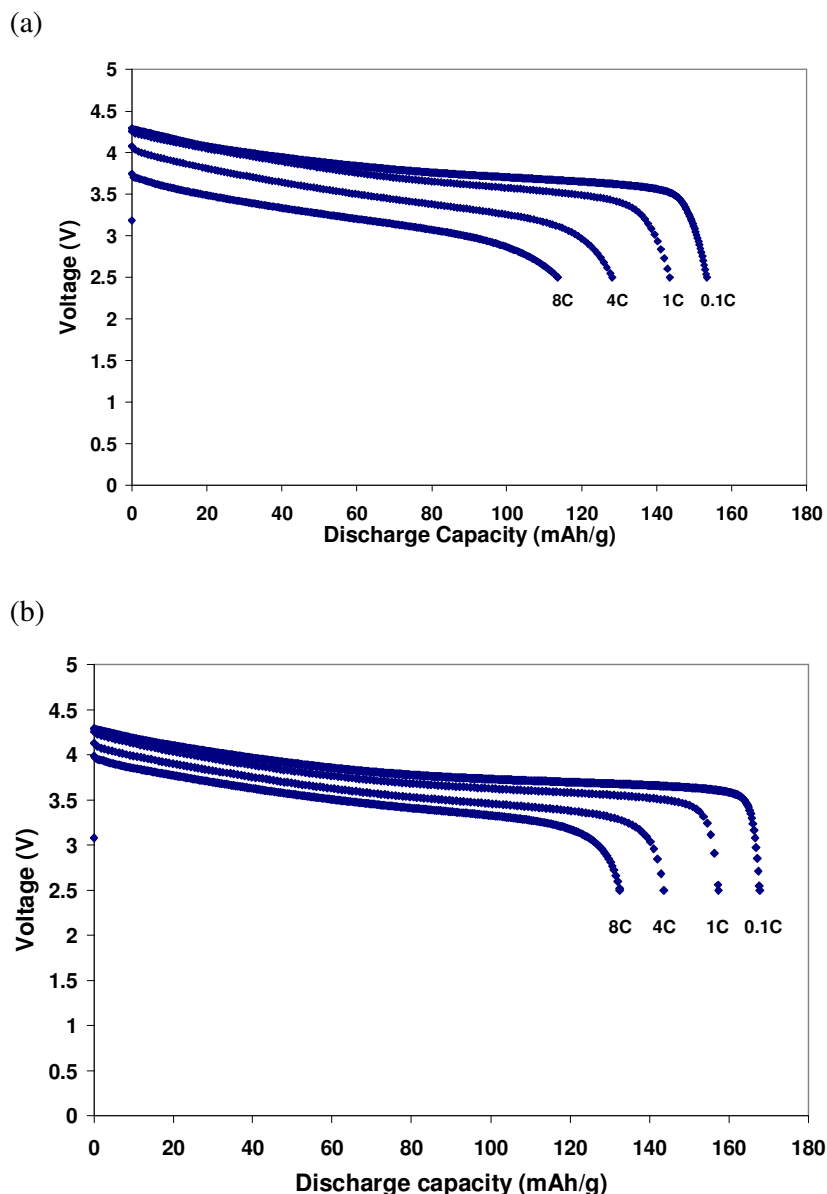


Figure 3. Rate capability of (a) HG- $\text{Li}_{1.02}\text{Ni}_{0.4}\text{Co}_{0.2}\text{Mn}_{0.4}\text{O}_2$, and (b) BM- $\text{Li}_{1.02}\text{Ni}_{0.4}\text{Co}_{0.2}\text{Mn}_{0.4}\text{O}_2$ cathodes.

Electrochemical characterization was carried out with coin-type cell. The electrode was prepared by using HG- and BM- $\text{Li}_{1.02}\text{Ni}_{0.4}\text{Co}_{0.2}\text{Mn}_{0.4}\text{O}_2$ / carbon [80% active material, 10% carbon black (TIMCAL)], and 10 wt% PVDF (alfa-aesar) as binder, dissolved in N-methyl-2-pyrrolidinone (NMP) solvent. The obtained slurry was then cast on the Al current collector and dried for 2h in an oven at 100°C. The resulting electrode film was subsequently pressed and punched into a circular disc. The thickness and loading of the electrode film were 40 μm and 6.0 mg/cm^2 , respectively. The coin cell was fabricated using the lithium metal as a counter electrode. The electrolyte was 1M solution of LiPF_6 in a mixture 1:1 (v/v) of ethylene carbonate (EC) and diethyl carbonate (DEC). The separator

(Celgard) was soaked in an electrolyte for 24 h prior to use. Coin cell assembly was carried out in an argon-filled glove box by keeping both oxygen and moisture level less than 2 ppm. The charge–discharge measurements were performed using Arbin battery tester at different C-rates over a potential range between 2.5V and 4.3 V.

3. RESULTS AND DISCUSSION

XRD patterns of HG- and BM- $\text{Li}_{1.02}\text{Ni}_{0.4}\text{Co}_{0.2}\text{Mn}_{0.4}\text{O}_2$ samples are shown in Fig. 1a & b, respectively. All the diffraction peaks can be indexed as a layered oxide structure based on a hexagonal $\alpha\text{-NaFeO}_2$ structure (space group R3m). No impurities and secondary phases are observed in these figures. The intensity ratio $I(003)/I(104)$ was greater than 1.2 and two double peaks of (006)/(102) and (108)/(110) were split clearly, indicating that the samples were well-crystallized with ordered, layered structure. The XRD peaks of the ball-milled powder relatively broadened. It is generally known that XRD peak broadening is associated with a small crystallite size and/or lattice strain caused by structural defects such as dislocations or stacking faults [30]. Fig. 2a & b show the particle size and morphology of HG- and BM- $\text{Li}_{1.02}\text{Ni}_{0.4}\text{Co}_{0.2}\text{Mn}_{0.4}\text{O}_2$ samples, respectively. As can be seen in these figures, the particle size of the BM- $\text{Li}_{1.02}\text{Ni}_{0.4}\text{Co}_{0.2}\text{Mn}_{0.4}\text{O}_2$ is relatively smaller than that of HG- $\text{Li}_{1.02}\text{Ni}_{0.4}\text{Co}_{0.2}\text{Mn}_{0.4}\text{O}_2$. It is obvious that the particles were broken into smaller particles that subsequently were stuck back together to become hard agglomerates during the ball-milling process (Fig. 2b).

In order to evaluate the effect of ball milling on the rate capability of $\text{Li}_{1.02}\text{Ni}_{0.4}\text{Co}_{0.2}\text{Mn}_{0.4}\text{O}_2$, the cells were cycled in the voltage range 2.5V to 4.3V. Fig. 3 shows the discharge capacities of the HG- and BM- $\text{Li}_{1.02}\text{Ni}_{0.4}\text{Co}_{0.2}\text{Mn}_{0.4}\text{O}_2/\text{Li}$ cells as a function of C rate between 3.0 and 4.3 V vs Li. The cells were charged galvanostatically with a 0.1 C rate before each discharge testing, and then discharged at different C rates from 0.1 to 8 C rates (16–1280 mA/ g). Clearly, the BM- $\text{Li}_{1.02}\text{Ni}_{0.4}\text{Co}_{0.2}\text{Mn}_{0.4}\text{O}_2$ delivered a higher discharge capacity than the HG- $\text{Li}_{1.02}\text{Ni}_{0.4}\text{Co}_{0.2}\text{Mn}_{0.4}\text{O}_2$, at all the tested C rates as shown in Table-1. For example, HG- and BM- $\text{Li}_{1.02}\text{Ni}_{0.4}\text{Co}_{0.2}\text{Mn}_{0.4}\text{O}_2$ cathodes delivered 156 mAh/g and 167 mAh/g, respectively, at 0.1C. Although the HG- $\text{Li}_{1.02}\text{Ni}_{0.4}\text{Co}_{0.2}\text{Mn}_{0.4}\text{O}_2$ showed an abrupt discharge capacity at higher C-rate, the BM- $\text{Li}_{1.02}\text{Ni}_{0.4}\text{Co}_{0.2}\text{Mn}_{0.4}\text{O}_2$ electrode retained its higher discharge capacity. At 8C rate, the obtained discharge capacity of the BM- $\text{Li}_{1.02}\text{Ni}_{0.4}\text{Co}_{0.2}\text{Mn}_{0.4}\text{O}_2$ was about 80%, compared to that of a 0.1 C rate, while the HG- $\text{Li}_{1.02}\text{Ni}_{0.4}\text{Co}_{0.2}\text{Mn}_{0.4}\text{O}_2$ electrode showed capacity retention of only 74% at the same C rate. The discharge capacity values are shown in Table-1. The lower discharge capacity of HG- $\text{Li}_{1.02}\text{Ni}_{0.4}\text{Co}_{0.2}\text{Mn}_{0.4}\text{O}_2$ cathode, when compared to that of BM- $\text{Li}_{1.02}\text{Ni}_{0.4}\text{Co}_{0.2}\text{Mn}_{0.4}\text{O}_2$, was caused by high polarization (compare Fig. 3a and Fig. 3b) resulting from deteriorating electrical contact between the oxide and carbon particles. The improved rate capability is reasonably due to increase of lithium ion conductivity through a decrease in particle size of the $\text{Li}_{1.02}\text{Ni}_{0.4}\text{Co}_{0.2}\text{Mn}_{0.4}\text{O}_2$ material after ball milling as shown in Fig. 2b. The obtained results thus strongly support that ball milling of cathode material with carbon is very effective way to enhance capacity and rate capability.

Table 1.

C-rate	Discharge Capacity of $\text{Li}_{1.02}\text{Ni}_{0.4}\text{Co}_{0.2}\text{Mn}_{0.4}\text{O}_2$, mAh/g	
	Before Ball Milling	After Ball Milling
0.1C	156	167
1.0C	145	157
5.0C	131	144
8.0C	115	133

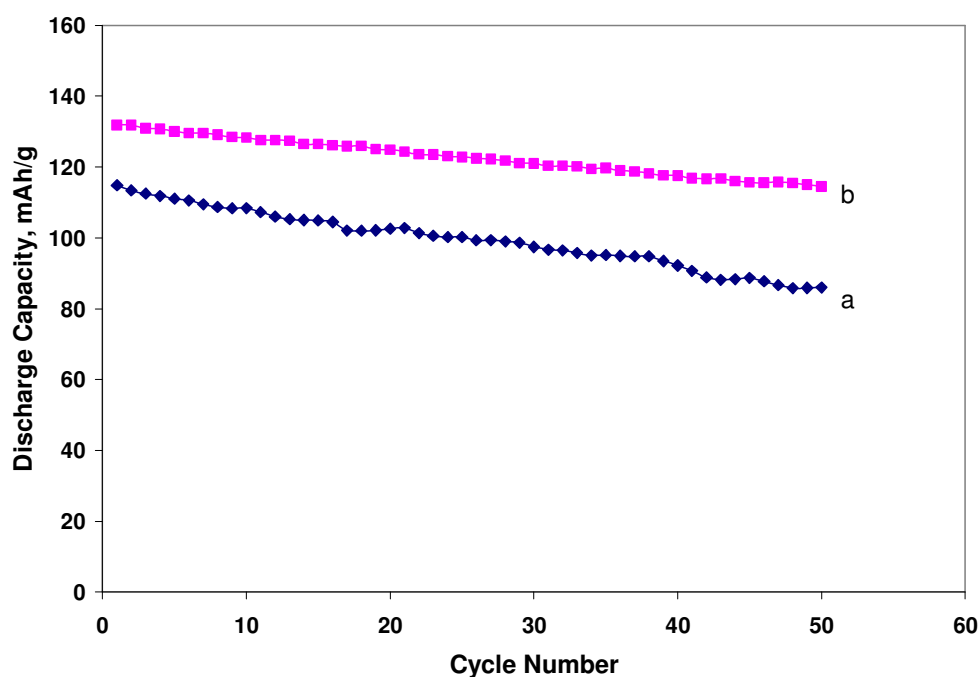


Figure 4. Cycling performance (half cell) of (a) HG- $\text{Li}_{1.02}\text{Ni}_{0.4}\text{Co}_{0.2}\text{Mn}_{0.4}\text{O}_2/\text{Li}$, and (b) BM- $\text{Li}_{1.02}\text{Ni}_{0.4}\text{Co}_{0.2}\text{Mn}_{0.4}\text{O}_2/\text{Li}$ cells at 8C-rate.

In order to observe the influence of the ball milling on cycling properties, HG- and BM- $\text{Li}_{1.02}\text{Ni}_{0.4}\text{Co}_{0.2}\text{Mn}_{0.4}\text{O}_2 / \text{Li}$ cells were assembled and the performance were measured at a current rate of 8C between 2.5 and 4.3 V. Fig. 4 indicates that the cycling performance of HG- and BM- $\text{Li}_{1.02}\text{Ni}_{0.4}\text{Co}_{0.2}\text{Mn}_{0.4}\text{O}_2$ electrode materials cycled at a high current rate of 8C. After 50 charge-discharge cycles, the BM- $\text{Li}_{1.02}\text{Ni}_{0.4}\text{Co}_{0.2}\text{Mn}_{0.4}\text{O}_2$ electrode exhibits excellent cycling performance with capacity retention ratio of about 87% when compared to that of HG- $\text{Li}_{1.02}\text{Ni}_{0.4}\text{Co}_{0.2}\text{Mn}_{0.4}\text{O}_2$ electrode which shows only 75% capacity retention ratio. Since the dendritic growth has been a very serious issue with Li metal anode during long term cycling, the cycling performance of HG- and BM- $\text{Li}_{1.02}\text{Ni}_{0.4}\text{Co}_{0.2}\text{Mn}_{0.4}\text{O}_2$ electrodes was also measured by assembling lithium-ion coin-cell with meso

carbon micro beads (MCMB) as anode. The cut-off voltage for the $\text{Li}_{1.02}\text{Ni}_{0.4}\text{Co}_{0.2}\text{Mn}_{0.4}\text{O}_2$ / MCMB cell was adjusted to 4.2 V because the lithium reversible intercalation into carbon occurs in the voltage range of 0-0.25 V. The assembled batteries are charged at a rate of 0.5C and discharged at 8C for 100 cycles between 2.5 and 4.2V. The BM- $\text{Li}_{1.02}\text{Ni}_{0.4}\text{Co}_{0.2}\text{Mn}_{0.4}\text{O}_2$ / carbon cell has capacity retention of 95 % after 100 cycles. HG- $\text{Li}_{1.02}\text{Ni}_{0.4}\text{Co}_{0.2}\text{Mn}_{0.4}\text{O}_2$ / carbon cell exhibited relatively poor capacity retention (80%) than that of BM- $\text{Li}_{1.02}\text{Ni}_{0.4}\text{Co}_{0.2}\text{Mn}_{0.4}\text{O}_2$ / carbon cell (95 %) as shown in Fig. 5.

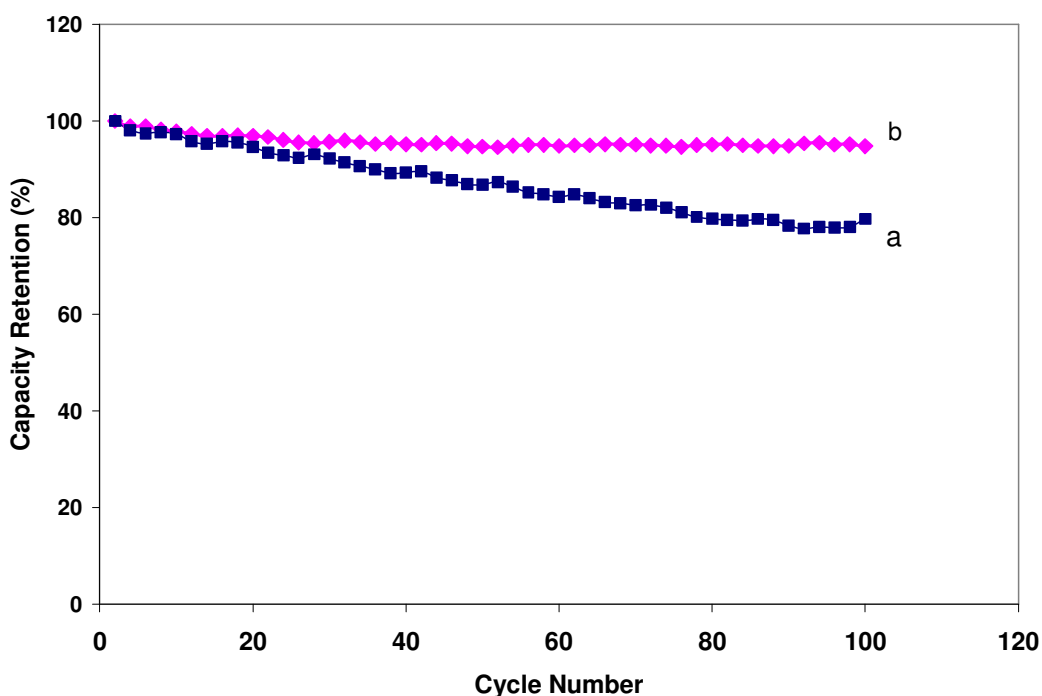
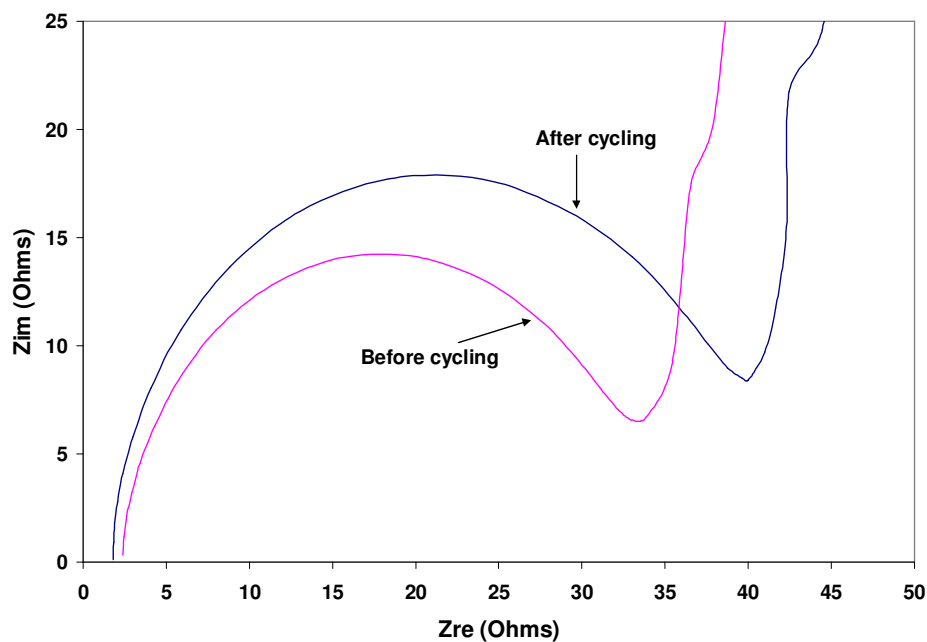


Figure 5. Cycling performance (full cell) of (a) HG- $\text{Li}_{1.02}\text{Ni}_{0.4}\text{Co}_{0.2}\text{Mn}_{0.4}\text{O}_2$ /carbon, and (b) BM- $\text{Li}_{1.02}\text{Ni}_{0.4}\text{Co}_{0.2}\text{Mn}_{0.4}\text{O}_2$ /Carbon cells at 8C-rate.

In general, the difference in battery performances would be related to the interfacial resistance between electrode and electrolyte. To explore the reason for the enhanced electrochemical performance, AC impedance measurements were carried out for the HG- and BM- $\text{Li}_{1.02}\text{Ni}_{0.4}\text{Co}_{0.2}\text{Mn}_{0.4}\text{O}_2$ / Li cells. Typical impedance spectra at the open-circuit voltage (OCV) for two fully charged cathodes are shown in Fig. 6. Generally, the semicircle in the high frequency range is related to effects arising from the resistance and capacitance of the electrolyte/electrode interface. The semicircle in the middle frequency range indicated the charge transfer resistance. The inclined line in the lower frequency represented the Warburg impedance, which is associated with Li-ion diffusion into the host particles. The initial diameters of semi-circle were nearly the same for both the cathodes. After charging, the diameter of the semi-circle increased significantly for the HG- cathode (Fig. 6a), but was relatively very low for the cathode ball milled with carbon (Fig. 6b). The charge transfer resistance of the HG- and BM- $\text{Li}_{1.02}\text{Ni}_{0.4}\text{Co}_{0.2}\text{Mn}_{0.4}\text{O}_2$ were 40 and 34 Ohms, respectively, after charge and discharge cycling at 8C. This is a clear indication of the significant decrease in cathode resistance

due to an improved contact between $\text{Li}_{1.02}\text{Ni}_{0.4}\text{Co}_{0.2}\text{Mn}_{0.4}\text{O}_2$ and carbon. Thus, the impedance results clearly support the enhanced electrochemical properties of the ball milled $\text{Li}_{1.02}\text{Ni}_{0.4}\text{Co}_{0.2}\text{Mn}_{0.4}\text{O}_2$ material such as capacity, rate capability, and cycleability.

(a)



(b)

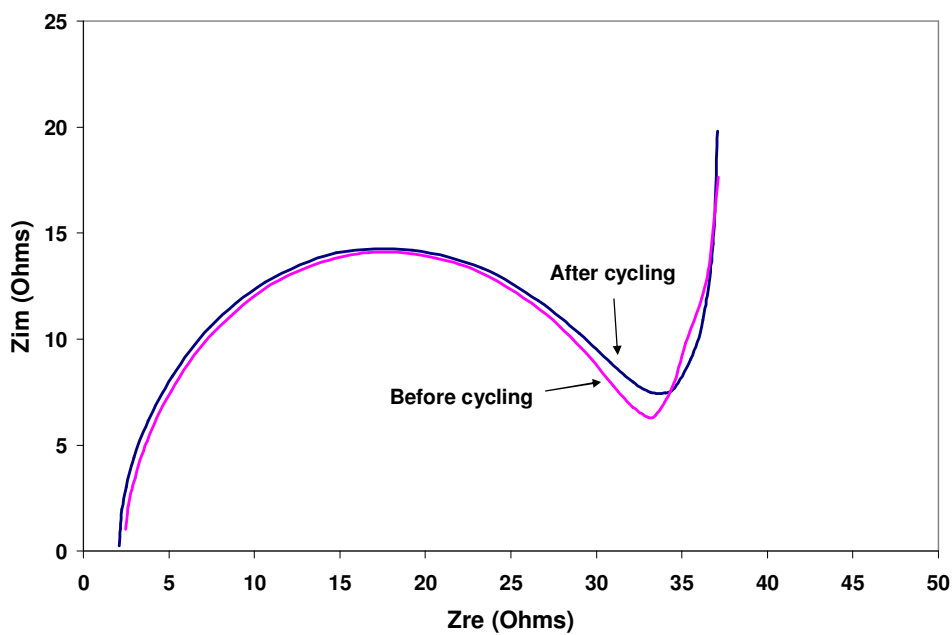


Figure 6. Electrochemical impedance spectra of (a) HG- $\text{Li}_{1.02}\text{Ni}_{0.4}\text{Co}_{0.2}\text{Mn}_{0.4}\text{O}_2$, and (b) BM- $\text{Li}_{1.02}\text{Ni}_{0.4}\text{Co}_{0.2}\text{Mn}_{0.4}\text{O}_2$ cathodes before and after cycling at 8C-rate.

4. CONCLUSIONS

In summary, layered $\text{Li}_{1.02}\text{Ni}_{0.4}\text{Co}_{0.2}\text{Mn}_{0.4}\text{O}_2$ materials were prepared by citric acid assisted sol gel method and their electrochemical performance was investigated by charge / discharge and electrochemical impedance spectroscopy. The capacity, rate capability and cycling performance of ball milled $\text{Li}_{1.02}\text{Ni}_{0.4}\text{Co}_{0.2}\text{Mn}_{0.4}\text{O}_2$ sample were significantly better than that of hand ground sample. From our experimental results, it is reasonable to suggest that ball milling enhances the electrochemical performance of layered $\text{Li}_{1.02}\text{Ni}_{0.4}\text{Co}_{0.2}\text{Mn}_{0.4}\text{O}_2$ cathode due to the decrease in contact resistance between oxide and carbon particles and increase of lithium ion conductivity through a decrease in the particle size of the active material. The results in this work suggest a simple and effective processing procedure to enhance the electrochemical performance of cathodes for rechargeable lithium batteries.

ACKNOWLEDGEMENTS

This work is supported by U.S-DOD-ARO-Electrochemistry and Advanced Energy Conversion Division under the grant # W911NF-08-C-0415 (Proposal No: 52322-CH-H (BOBBA)). BRB and R. Santhanam thank Dr. Robert Mantz for supporting cathode materials research for developing hybrid energy storage devices.

References

1. T. Nagaura, *Prog. Batteries Battery Mater.*, 10 (1991) 218
2. K. Mizushima, P.C. Jones, P.J. Wiseman, J.B. Goodenough *Mater. Res. Bull.*, 15 (1980) 783.
3. Y.M. Choi, S.I. Pyun, S.I. Moon *Solid State Ionics*, 89 (1996) 43.
4. J. Jiang, J.R. Dahn, *Electrochem Commun.*, 6 (2004) 39.
5. G.G. Amatucci, J.M. Tarascon, L.C. Klein *Solid State Ionics* 83 (1996)167.
6. S.T. Myung, N. Kumagai, S. Komaba, H.T. Chung, *Solid State Ionics*, 139 (2001) 47
7. T. Ohzuku, Y. Makimura *Chem. Lett.*, 30 (2001) 642.
8. T. Ohzuku, Y. Makimura, *Chem. Lett.*, 30 (2001) 744.
9. B. J. Hwang, Y.W. Tsai, D. Cariler, G. Ceder *Chem. Mater.*, 15 (2003) 376.
10. Y.W. Tsai, B.J. Hwang, G. Ceder, H.S. Sheu, D.G. Liu, J.F. Lee *Chem. Mater.*, 17 (2005) 3191.
11. S.H. Park, C.S. Yoon, S.G. Kang, H.S. Kim, S.I. Moon, Y.K. Sun *Electrochim. Acta*, 49 (2004) 557.
12. J. Cho, A. Manthiram *J. Electrochem. Soc.*, 152 (2005) A1714
13. S.K. Hu, G.H. Cheng, M.Y. Cheng, B.J. Hwang, R. Santhanam, *J. Power Sources*, 188 (2009) 564
14. B.J. Hwang, T.H. Yu, M.Y. Cheng, R. Santhanam *J. Mater. Chem.*, 19 (2009) 4536.
15. S.W. Woo, S.T. Myung, H. Bang, D.W. Kim, Y.K. Sun *Electrochim Acta* 54 (2009) 3851.
16. F. Zhou, X. Zhao, J.R. Dahn *J. Electrochem Soc.*, 156 (2009) A343
17. Y. Chen, R. Chen, Z. Tang, L. Wang, *J. Alloys Compd.*, 476 (2009) 539.
18. J.D. Wilcox, S. Patoux, M.M. Doeff, *J. Electrochem.Soc.*, 156 (2009) A192.
19. S. Sivaprakash, S.B. Majumder *J. Alloys Compd.* 479 (2009) 561.
20. B. Zhang, G. Chen, Y. Liang, P. Xu, *Solid State Ionics*, 180 (2009) 398.
21. L. Liu, K. Sun, N. Zhang, T. Yang *J. Solid State Electrochem.*, 13 (2009) 1381.
22. S.T. Myung, K. Izumi, S. Komaba, Y.K. Sun, H. Yashiro, N. Kumagai, *Chem Mater.*, 17 (2005) 3695.
23. Z. Zhang, Z. Gong, Y. Yang, *J. Phys. Chem B*, 108 (2004) 17546.
24. S.M. Lee, S.H. Oh, W.I. Cho, H. Jang, *J Power Sources* 52 (2006) 1507.

25. Y. Wu, A.V. Murugan, A. Manthiram *J. Electrochem. Soc.*, 55 (2008) A635.
26. Z. Liu, A. Yu, J.Y. Lee *J Power Sources*, 74 (1998) 228.
27. S.H. Kang, J.B. Goodenough, L.K. Rabenberg *Chem. Mater.*, 13 (2001) 1758.
28. B.J. Hwang, R. Santhanam, D.G. Liu *J. Power Sources*, 97-98 (2001) 443.
29. B.J. Hwang, R. Santhanam, D.G. Liu, *J. Power Sources*, 101 (2001) 86.
30. Y.I. Jang, B. Huang, H. Wang, D.R. Sadoway, Y.M. Chiang, *J Electrochem Soc.*, 146 (1999) 3217.